



# EFFECT OF GOLD NANOPARTICLES AND ELECTRODE DRYING TIME ON REDUCED GRAPHENE OXIDE-BASED COMPOSITE WITH RESPECT TO PEAK CURRENT OF CYCLIC VOLTAMMETRY

Habibah Farhana Abdul Guthoos<sup>1</sup>, Nik Nurfaten Noorin<sup>1</sup>, Nur Alya Batrisya Ismail<sup>1</sup>, Afidalina Tumian<sup>2</sup>  
and Wan Wardatul Amani Wan Salim<sup>1</sup>

<sup>1</sup>Department of Biotechnology, Faculty of Engineering, International Islamic University Malaysia, Gombak, Kuala Lumpur, Malaysia

<sup>2</sup>Department of Computer Science, Faculty of Information and Communication Technology, International Islamic University Malaysia, Gombak, Kuala Lumpur, Malaysia

E-Mail: [asalim@iium.edu.my](mailto:asalim@iium.edu.my)

## ABSTRACT

Screen-printed glassy carbon electrodes (GCEs) 2 mm in diameter deposited with composites of reduced graphene oxide-gold nanoparticles (rGO-AuNPs), reduced graphene oxide-cellulose (rGO-cellulose), and reduced graphene oxide-gold nanoparticles-cellulose (rGO-AuNPs-cellulose) were characterized in terms of the effect of drying time on the peak oxidative current and surface roughness. From the cyclic voltammetry (CV) graph, at 12 hrs of electrode drying time in ambient air the rGO-AuNPs/GCE showed the highest anodic peak current of 1252.82  $\mu\text{A}$ , in comparison to the rGO-cellulose/GCE with the lowest at 24.64  $\mu\text{A}$ . FESEM results show that the rGO-AuNPs composite has the roughest surface morphology as well. Furthermore, there seem to be two layers of surface morphology in cellulose-based samples. The results obtained suggest that rGO-AuNPs/GCEs with 12 hours drying time have the highest peak current and the largest surface area owing to its roughness, thus implying that rGO-AuNPs has the most electrode area involved in redox reactions. The results also suggest the rGO-AuNPs nanocomposite can be effective as a sensitive transducer material for an electrochemical biosensor.

**Keywords:** cyclic voltammetry, graphene, gold nanoparticle, reduced graphene oxide, cellulose.

## 1. INTRODUCTION

A biosensor can be defined as a compact analytical device incorporating a biological or biologically derived recognition element that is integrated with a physico-chemical transducer [1-2]. Biosensors can be used to detect a wide range of analytes [1] with good sensitivity and selectivity; they have been applied in food safety and security [3-5], public health [6-8], and environmental safety [9-11]. There are three main components of an electrochemical biosensor: the biological recognition element that differentiates the target molecules in the presence of background chemicals, transducer that converts the interaction of the recognition element and the targeted analytes into a measurable electrical signal, and a signal-processing and hardware system that displays the measured electrical signal in a readable form [12].

In this research, we focus on understanding the transducer component of a biosensor; improvements in the transducer layer can enhance sensor performance in terms of sensitivity, selectivity, and detection limit. Nanomaterials have been known to improve the performance of the transducer layer and thus the performance of an electrochemical biosensing device [13-15]. The incorporation of nanomaterials into transducers can increase the effective surface area of the electrode for electrochemical redox reactions, contributes to improved electron transfer from the bioreceptor, and subsequently leads to improvements in signal detection [16]. Being the unrolled version of a carbon nanotube [17-20], graphene and its composites have potential as a transducer layer thanks to their structure, where every atom can be involved in chemical reactions, increasing graphene

chemical reactivity. Furthermore, the planar structure makes it extremely attractive as a support material for metal oxides and polymer materials [21]. However, graphene lacks electrocatalytic ability, especially graphene in the form of graphene oxide (GO); GO has an abundance of oxygenated functional groups, making GO act as an insulator. Therefore, for GO to be part of a sensitive electrochemical biosensor, it must be incorporated with nanoparticles, such as gold nanoparticles (AuNPs), with high electrocatalytic property. In addition to incorporation of AuNPs, GO can be electrochemically reduced in acid to increase its conductivity; reduced graphene oxide (rGO) has conductivity similar to that of pristine graphene but with more defect sites for housing AuNPs [22, 23].

AuNPs can facilitate the transfer of electrons between less conductive materials and improve electron transfer [24, 25]. An rGO-AuNPs hybrid nanocomposite can provide additional properties of higher effective surface area, increased electrocatalytic activity [26], improved electrical conductivity and water solubility, and biocompatibility for the immobilization of a biorecognition element. To test the synergistic properties of rGO-AuNPs, we incorporated non-electrocatalytic materials such as cellulose [27] to verify the effect of combining AuNPs with graphene. Cellulose is the most abundant natural polymer in nature and is biodegradable and biocompatible [27]. Cellulose is not easily dissolved in common solvents and has strong intermolecular hydrogen bonds with a high degree of polymerization and crystallinity [28, 29]. Furthermore, to bind AuNPs with graphene, Nafion<sup>®</sup> is often used to help in the shuttle of ions from the measurement solution across the



transduction layers [30]. Although Nafion<sup>®</sup> and conductive polymers were often used as binders for various nanomaterial composites for electrochemical sensing, it is interesting to see the effect of other polymers as binders, especially those without the ion shuttling capability of Nafion<sup>®</sup>. Figure-1 shows the rGO-based composites used in this study.

In this preliminary work, we studied the effect of incorporating AuNPs with rGO on the electrocatalytic

ability of the nanocomposite, and also looked at the effect of nanocomposite-based electrode drying time on cyclic voltammetry peak current. We also used cellulose as a control material to impede electron transfer, and field-emission electron microscope (FESEM) to verify the electrochemical results by looking into the morphology of the rGO-AuNPs nanocomposites with and without cellulose.

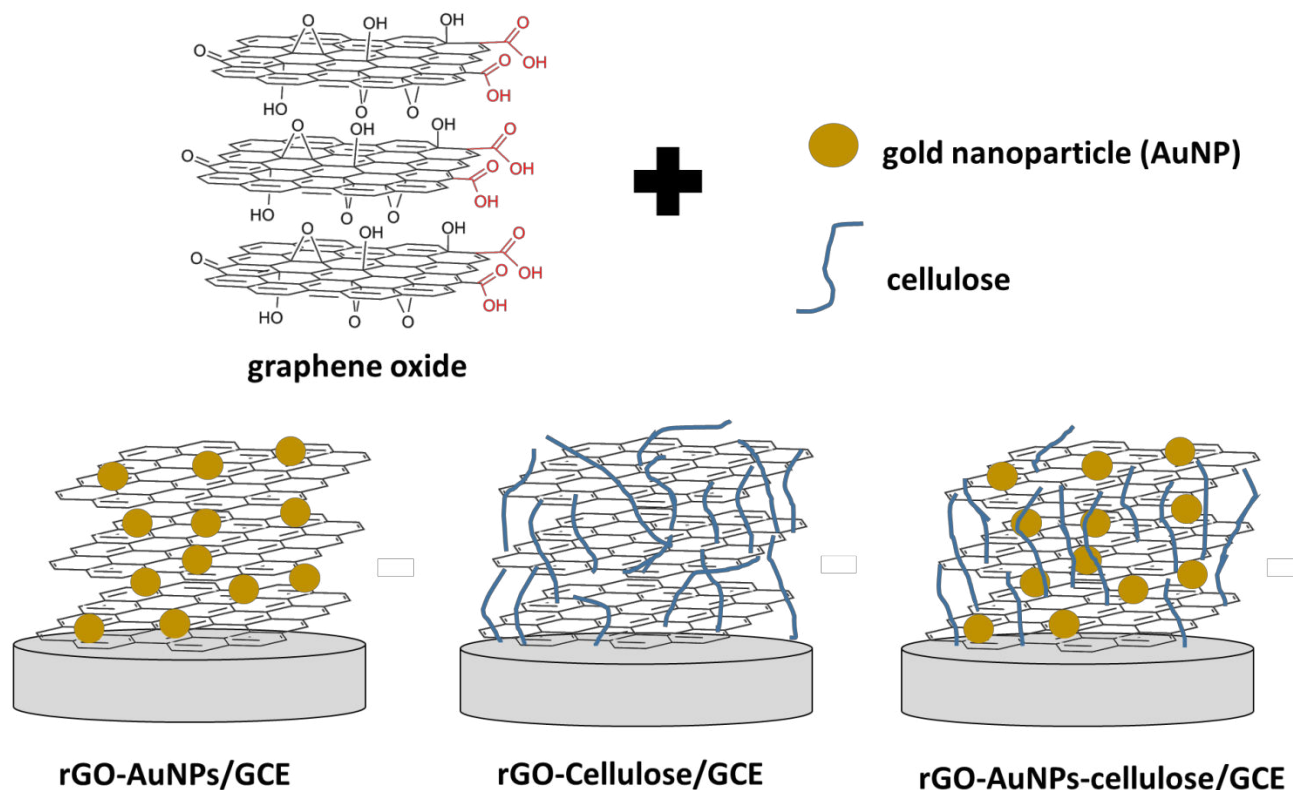


**Figure-1.** Schematic of composites of reduced graphene oxide-gold nanoparticles (rGO-AuNPs), reduced graphene oxide-cellulose (rGO-cellulose), and reduced graphene oxide-gold nanoparticles-cellulose (rGO-AuNPs-cellulose) on glassy carbon electrode (GCE).

## 2. MATERIALS AND METHODS

### 2.1 Materials and reagents

Gold nanoparticles (AuNPs) 15 nm in diameter ( $1.64 \times 10^{12}$  particles/ml) was purchased from Sigma-Aldrich, St. Louis, MO, USA. Ultra-highly concentrated single-layer graphene oxide (UHC GO), 6.2 mg/ml, was purchased from Graphene Supermarket (<https://graphene-supermarket.com>), USA. Screen-printed glassy carbon electrodes (GCEs) were purchased from Pine Instruments, Grove City, Pennsylvania, USA. Potassium ferricyanide ( $K_3Fe(CN)_6$ ) was purchased from R&M Chemicals, Selangor, Malaysia. Potassium dihydrogen phosphate ( $KH_2PO_4$ ) and disodium hydrogen phosphate ( $Na_2HPO_4$ ), obtained from Sigma-Aldrich, St. Louis, MO, USA, were used to prepare 0.1 M PBS, pH 5. Deionized (DI) water was used throughout the experiments, unless otherwise stated.

### 2.2 Electrochemical reduction and characterization

Electrochemical reduction and characterization of reduced graphene-based composites as transducer material were performed using a three-electrode cell and a portable potentiostat called pocket STAT (IVIUM Technologies, Eindhoven, the Netherlands). The electrochemical reduction was conducted on the electrode using repetitive cyclic voltammetry (CV) with potential range from 0 V to -1.5 V at 0.1 V/s in 0.05 M PBS, pH 5.0, for 30 cycles. The rGO-AuNPs/GCE was rinsed with DI water and dried at room temperature. Finally, CVs were performed on the rGO-AuNPs/GCE in a redox-active solution of 0.1 M potassium ferricyanide ( $K_3Fe(CN)_6$ ), and the oxidation-reduction capability was determined via the CV oxidative peak current.



### 2.3 Deposition method for rGO-AuNPs/GCE, rGO-cellulose/GCE, and rGO-AuNPs-cellulose/GCE

For fabrication of an rGO-AuNPs/GCE, 500  $\mu$ l of AuNPs was mixed with 2 ml ultra-highly concentrated GO solution. This solution was stirred using an electric stirrer and sonicated at 30  $^{\circ}$ C for 10 min in order to form a well-mixed GO and AuNPs mixture. Then 3  $\mu$ l of this mixture were drop-cast onto a GCE [31]. The electrode was dried at room temperature. Afterwards, the electrode was reduced and characterized.

For fabrication of an rGO-cellulose/GCE, 2 ml highly concentrated GO solution (6.2 mg/ml) was mixed with 1000  $\mu$ l of 1 M cellulose in DI. The composite formed was stirred with an electric stirrer and sonicated at 30  $^{\circ}$ C for 10 min. Next 3  $\mu$ l of the composite mixture was drop-cast onto a GCE and dried at room temperature. Afterwards, the electrode was reduced and characterized.

For fabrication of an rGO-AuNPs-cellulose/GCE, 2 ml highly concentrated GO solution was mixed with 500  $\mu$ l AuNPs and 1000  $\mu$ l of 1 M cellulose in DI. The composite formed was stirred by an electric stirrer and sonicated at 30  $^{\circ}$ C for 10 min. Then 3  $\mu$ l of the composite mixture was drop-cast onto a GCE and dried at room temperature. Afterwards, the electrode was reduced and characterized.

### 2.4 Electrode drying time

To study the effect of drying time on the electrode anodic peak current, samples were dried for 2, 4, 6 or 12 hrs in ambient air after deposition on electrodes. CV measurements were conducted after each drying time. Note here that for each drying time, a new sample was prepared as described in section 2.3.

### 2.5 Preparation of electrodes for FESEM and characterization of composite surface morphology

Three samples with 12-hr drying time were selected for discussion purposes: rGO-AuNPs/GCE, rGO-cellulose/GCE, and rGO-AuNPs-cellulose/GCE. We chose these samples based on the oxidative current from CV measurements that showed significant differences in terms of current magnitude compared to the bare electrodes. Surface morphology of these samples was examined using FESEM (Hitachi S-4800) at MIMOS Sdn. Bhd, Seri Kembangan, Malaysia. To avoid charging of the composites, all samples on the electrodes were coated with a thin layer of platinum before entering the FESEM machine.

### 2.6 Statistical testing used to evaluate significance of peak current

Statistical testing was conducted to look for significant differences in the measured current during forward scan across four experimental settings (i.e., bare GCE, rGO-AuNPs/GCE, rGO-cellulose/GCE, and rGO-AuNPs-cellulose/GCE). As explained in Section 2.4, the experiments were repeated at four different drying times; 2, 4, 6, and 12 hours. Two regions were chosen: from -0.50 V to 1.00 V (region A) and from 0.13 V to 0.61 V (region B) on the CV graphs.

Previous checks on similar data have shown that the variance across samples differs significantly different (unpublished data). Therefore, the nonparametric Kruskal-Wallis statistical test was chosen for peak current. In cases where significant differences were observed, a post-hoc testing was carried out to perform pair wise comparisons in order to indicate which experiment setting is significantly different from which. In this work, Dunn's test was applied with  $p$ -values adjusted using the Bonferroni method. Results are significant when the  $p$ -values are  $p < 0.05$  and  $p < 0.01$ .

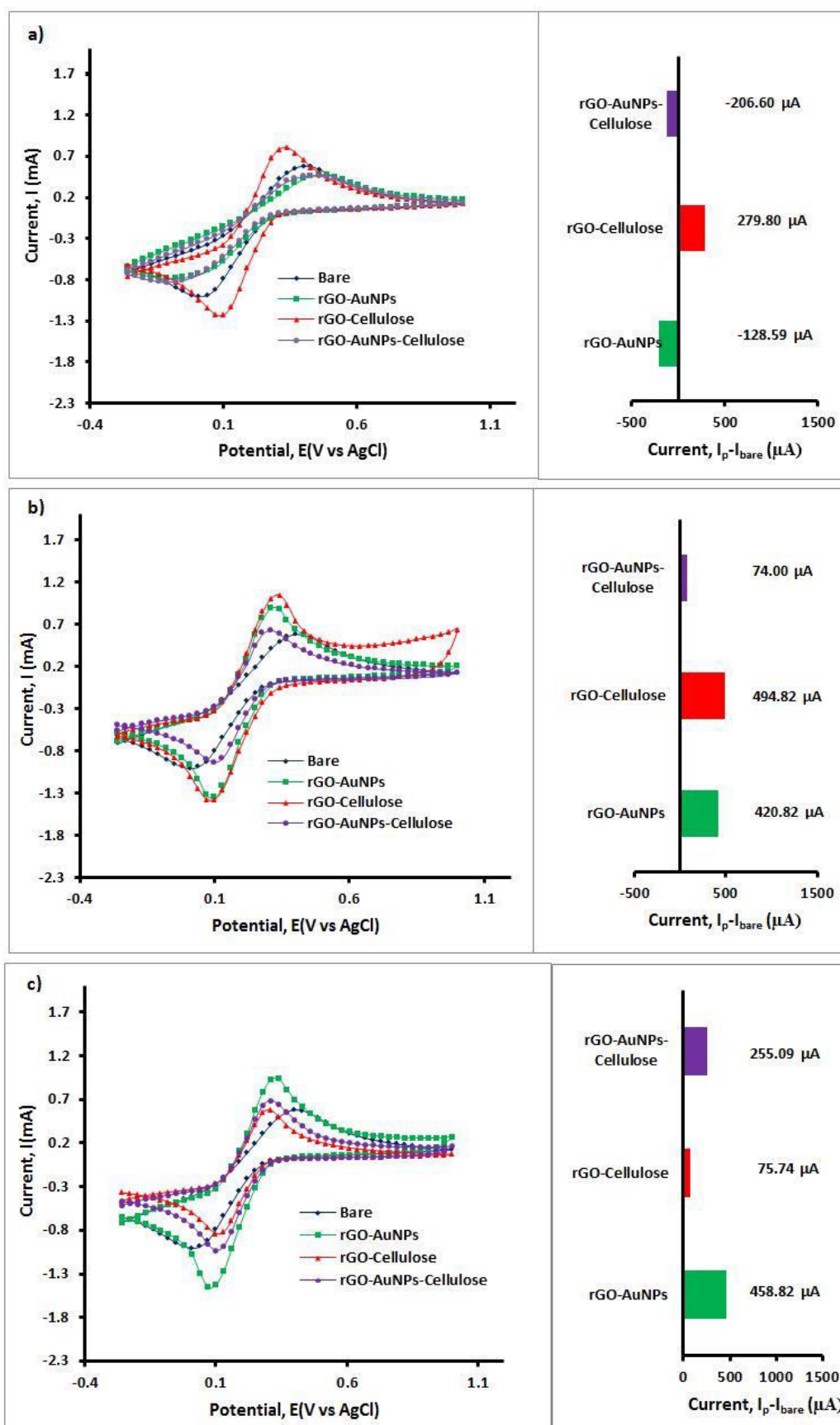
## 3. RESULTS AND DISCUSSIONS

### 3.1 Electrochemical characterization of electrode

Figure-2 a-d shows the cyclic voltammetry (CV) curves for bare/unmodified glassy carbon electrode (GCE), rGO-AuNPs/GCE, rGO-cellulose/GCE, and rGO-AuNPs-cellulose/GCE and the respective bar graphs for the difference in peak current from the bare GCE at 2, 4, 6 and 12 hrs respectively. The negative peak current indicates that the peak current from the modified electrode is lower than that of the bare. At 2 hrs, both the rGO-AuNPs and rGO-AuNPs-cellulose samples showed a lower peak current than did the bare, whereas the rGO-cellulose sample did not. Interestingly, the rGO-cellulose - based samples have a higher peak current compared to samples with AuNPs for 2 and 4 hrs drying time. This trend is reversed at longer drying time (6 and 12 hrs); peak currents of GCEs with AuNPs have higher peak currents than the bare.

GCEs modified with rGO-AuNPs showed higher peak current at 12 hrs drying time (1252.82  $\mu$ A) than do the other modified electrodes (252.36  $\mu$ A for rGO-AuNPs-cellulose/GCE and 24.64  $\mu$ A for rGO-cellulose/GCE), suggesting the higher electrocatalytic activity of rGO-AuNPs/GCEs towards  $K_3Fe(CN)_6$  solution. The high CV anodic peak current also indicates the high conductivity and low internal resistance of rGO-AuNPs composites. The higher anodic peak current can be a result of the high conductivity and electrocatalytic ability of AuNPs [25]. AuNPs act as electron-transfer mediators or as electrical wires, allowing the proper tunnelling of electrons. In addition, graphene has good affinity for the electrode surface, and its conductive network promotes the electron transfer between the  $K_3Fe(CN)_6$  solution and the electrode surface [14]. Furthermore, owing to the insulative property of cellulose, a longer drying time for cellulose-based samples can suggest better attachment of the cellulose to the electrodes, allowing the cellulose layer to impede electron transfer.

Testing for significant comparisons for all electrode samples with respect to the bare samples at both regions A and B resulted in  $p$ -values of more than 0.05, indicating that these results are not statistically significant. Interestingly, the only significant result is between rGO-AuNPs/GCE and rGO-cellulose/GCE at 12 hrs drying time at region B. This is supportive of the results; only at 12 hrs are both electrodes at their highest and lowest peak current, respectively, and  $p < 0.01$ .





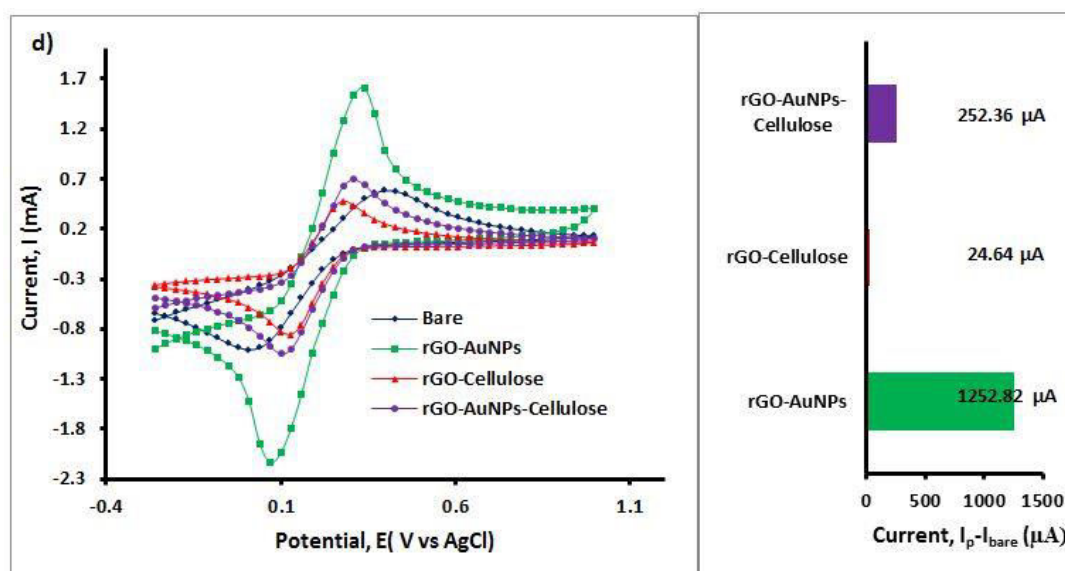


**Figure-2.** Cyclic voltammetry graphs of all composites with respective bar graphs for the difference in anodic peak current from the bare peak current for (a) 2, (b) 4, (c) 6, and (d) 12 hrs of electrode drying time.

### 3.2 Surface morphology of composites

Figure-3 shows the FESEM images at 10 X magnification for a) rGO-AuNPs, b) rGO-AuNPs-cellulose, and c) rGO-cellulose at 12 hrs drying time. The figure clearly shows that the rGO-AuNPs have the roughest surface morphology compared to the other samples. In addition, both cellulose-containing samples seem to show two layers of morphology, with a rougher

one beneath a smoother surface, suggesting that cellulose does not mix well with the GO. From the results we conclude that an rGO-AuNPs/GCE with a drying time of 12 hours is more effective for electrochemical sensors owing to the highest peak current compared to the bare electrode and a rougher surface for effective electron transfer.

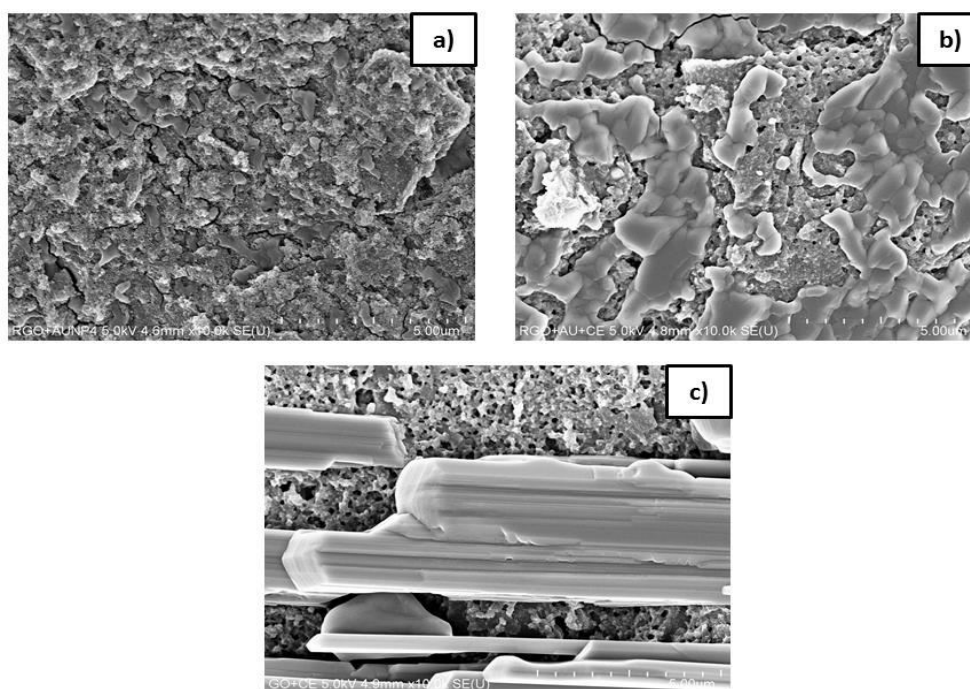


**Figure-3.** FESEM images at 10 X of samples at 12 hrs drying time. a) rGO-AuNPs, b) rGO-AuNPs-cellulose, c) rGO-cellulose.



#### 4. CONCLUSIONS

In this preliminary study, CV characterization of transducer layers of rGO-AuNPs, rGO-cellulose, and rGO-AuNPs-cellulose was conducted to determine the oxidative peak current, and FESEM was used to correlate the results with the surface roughness of the composites on GCEs. From the results, it appears that rGO-AuNPs electrodes with 12 hours of drying time are more effective materials for electrochemical biosensors owing to the highest peak current that can enable sensitive transduction of biological signals, and the roughest surface that enables faster electron transfer and better attachment of biomolecules for biosensing purposes. This outcome demonstrates that the drying time of the nanocomposite can influence the transducer performance; the choice of transduction material is critical to developing biosensors with high sensitivity, low detection limit, stability, low noise and signal artifacts, and longer lifetime. More studies are needed to characterize the transducer layer and to optimize the transduction.

#### ACKNOWLEDGEMENTS

This material for the work was funded by the Malaysia Ministry of Higher Education (MoHE) Research Acculturation Grant Scheme (RAGS14-038-0101) and payment for publication was funded by IIUM Research Initiative Grant Scheme (RIGS16-355-0519), both awarded to Dr. Wan Wardatul Amani Wan Salim. We would like to thank MIMOS Sdn. Bhd. for their help with the FESEM imaging.

#### REFERENCES

- [1] Arris F.A. Characterization of electrochemical transducer for biosensor application. unpublished.
- [2] Arris F.A. 2016. Optimization and Characterization of Graphene Nanocomposites for Glucose Biosensors. MSc. Thesis, Dept. of Biotechnology Engineering, International Islamic University Malaysia (IIUM).
- [3] Goriushkina T. B., Soldatkin, A. P., and Dzyadevych, S. V. 2009. Application of amperometric biosensors for analysis of ethanol, glucose, and lactate in wine. *Journal of Agricultural and Food Chemistry*. 57(15): 6528-6535.
- [4] Laube T., *et al.* 2011. Magneto immunosensor for gliadin detection in gluten-free foodstuff: Towards food safety for celiac patients. *Biosensors and Bioelectronics*. 27(1): 46-52.
- [5] Scognamiglio V., *et al.* 2014. Biosensing technology for sustainable food safety. *Trends in Analytical Chemistry*. 62, pp. 1-10.
- [6] Cordeiro M., *et al.* 2016. Gold nanoparticles for diagnostics: Advances towards points of care. *Diagnostics*. 6(4): 43.
- [7] He J. L., *et al.* 2013. An electrochemical immunosensor based on gold nanoparticle tags for picomolar detection of c-Myc oncoprotein. *Sensors and Actuators B: Chemical*. 181, pp. 835-841.
- [8] Dai Z., *et al.* 2009. Immobilization and direct electrochemistry of glucose oxidase on a tetragonal pyramid-shaped porous ZnO nanostructure for a glucose biosensor. *Biosensors and Bioelectronics*. 24(5): 1286-1291.
- [9] Hayat A. and Marty J. L. 2014. Disposable screen printed electrochemical sensors: Tools for environmental monitoring. *Sensors*. 14(6): 10432-10453.
- [10] Gilbert L., *et al.* 2011. Development of an amperometric, screen-printed, single-enzyme phosphate ion biosensor and its application to the analysis of biomedical and environmental samples. *Sensors and Actuators B: Chemical*. 160(1): 1322-1327.
- [11] Dostálék J., *et al.* 2006. SPR biosensors for detection of biological and chemical analytes. *Chemical Sensors and Biosensors*. 4, pp. 177-190.
- [12] Guthoos H. F. A. 2016. Development of Graphene-Based Transducer Layer for Biosensor. MSc. Thesis, Dept. of Biotechnology Engineering, International Islamic University Malaysia (IIUM). Unpublished.
- [13] Devi N.B. 2015. An overview of fabricating nanostructured electrode materials for biosensor applications. *International Journal of Electrochemical Science*. 10, pp. 8607-8629.
- [14] Singh R.P. 2011. Prospects of nanobiomaterials for biosensing, *International Journal of Electrochemistry*. pp. 1-30.
- [15] Wild S., *et al.* 2004. Global prevalence of diabetes: estimates for the year 2000 and projections for 2030. *Diabetes Care*, 27(5), pp. 1047-53.
- [16] Saei A.A., *et al.* 2013. Electrochemical biosensors for glucose based on metal nanoparticles. *Trends in Analytical Chemistry*, 42, pp. 216-227.



- [17] Novoselov K.S., *et al.* 2005. Two-dimensional gas of massless Dirac fermions in graphene. *Nature*. 438(7065): 197-200.
- [18] Xiao Y. and Li C.M. 2008. Nanocomposites: from fabrications to electrochemical bioapplications. *Electroanalysis*. 20(6): 648-662.
- [19] Singh V., *et al.* 2011. Graphene based materials: past, present and future. *Progress in Materials Science*. 56(8): 1178-1271.
- [20] Yang J. and Gunasekaran S. 2013. Electrochemically reduced graphene oxide sheets for use in high performance supercapacitors. *Carbon*. 51, pp. 36-44.
- [21] Kou R., *et al.* 2011. Stabilization of electrocatalytic metal nanoparticles at metal - metal oxide - graphene triple junction points. *Journal of the American Chemical Society*. 133(8): 2541-2547.
- [22] Pei S. and Cheng H. M. 2012. The reduction of graphene oxide. *Carbon*. 50(9): 3210-3228.
- [23] Liu E. And Zhang X. 2014. Electrochemical sensor for endocrine disruptor bisphenol A based on a glassy carbon electrode modified with silica and nanocomposite prepared from reduced graphene oxide and gold nanoparticles. *Analytical Methods*. 6(21): 8604-8612.
- [24] Xiao Y. and Li C.M. 2008. Nanocomposites: from fabrications to electrochemical bioapplications. *Electroanalysis*. 20(6): 648-662.
- [25] Hebié S. T., *et al.* 2016. Size-dependent electrocatalytic activity of free gold nanoparticles for the glucose oxidation reaction. *Chemical Physics and Physical Chemistry*. 17(10): 1454-1462.
- [26] Dutta D., *et al.* 2014. SnO<sub>2</sub> quantum dots-reduced graphene oxide composite for enzyme-free ultrasensitive electrochemical detection of urea. *Analytical Chemistry*. 86(12): 5914-5921.
- [27] Zimmermann T., Bordeanu N. and Strub E. 2010. Properties of nanofibrillated cellulose from different raw materials and its reinforcement potential. *Carbohydrate Polymers*. 79(4): 1086-1093.
- [28] Tashiro K. and Kobayashi M. 1991. Theoretical evaluation of three-dimensional elastic constants of native and regenerated celluloses: role of hydrogen bonds. *Polymer*. 32(8): 1516-1526.
- [29] Weng Z., *et al.* 2011. Graphene-cellulose paper flexible supercapacitors. *Advanced Energy Materials*. 1(5): 917-922.
- [30] McGovern M.S., *et al.* 2003. Effects of Nafion as a binding agent for unsupported nanoparticle catalysts. *Journal of Power Sources*. 115, pp. 35-39.
- [31] Niu X., *et al.* 2013. Highly sensitive and selective dopamine biosensor based on 3, 4, 9, 10-perylene tetracarboxylic acid functionalized graphene sheets/multi-wall carbon nanotubes/ionic liquid composite film modified electrode. *Biosensors and Bioelectronics*, 41, pp. 225-231.
- [32] Yang J., *et al.* 2011. Electrochemical synthesis of reduced graphene sheet-AuPd alloy nanoparticle composites for enzymatic biosensing. *Biosensors and Bioelectronics*. 29(1): 159-166.
- [33] Shi J., *et al.* 2011. A comparative study of enzyme immobilization strategies for multi-walled carbon nanotube glucose biosensors. *Nanotechnology*. 22(35): 355502.